

1 **Brief Communication**

2 **Co-seismic displacement on October 26 and 30, 2016 (M_w 5.9 and 6.5) -**
3 **earthquakes in central Italy from the analysis of a local GNSS network**

4
5 De Guidi Giorgio^{1,2}, Vecchio Alessia¹, Brighenti Fabio¹, Caputo Riccardo^{3,4,5}, Carnemolla Francesco¹, Di Pietro
6 Adriano¹, Lupo Marco¹, Maggini Massimiliano^{3,5}, Marchese Salvatore¹, Messina Danilo¹, Monaco
7 Carmelo^{1,2}, Naso Salvatore¹

9 1) Department of Biological, Geological and Environmental Sciences, University of Catania, Italy

10 2) CRUST, UR-UniCT, Catania, Italy

11 3) Department of Physics and Earth Sciences, University of Ferrara, Italy

12 4) Research and Teaching Center for Earthquake Geology, Tyrnavos, Greece

13 5) CRUST, UR-UniFE, Ferrara, Italy

14 *Corresponding author: G. De Guidi (deguidi@unict.it)*

16 **1 - Abstract**

17 On August 24th 2016 a strong earthquake ($M_w = 6.0$) affected Central Italy starting an intense seismic
18 sequence. Field observations, DInSAR analyses, preliminary focal mechanisms as well as the distribution of
19 aftershocks suggested the reactivation of the northern sector of the Laga Fault, whose southern sector was
20 already reactivated during the 2009 L'Aquila sequence, and the southern segment of the Monte Vettore
21 Fault System (MVFS). Based on these preliminary information and following the stress-triggering concept
22 (Stein et al., 1999; Steacy et al., 2005), we tentatively identified a potential fault zone most vulnerable to
23 future seismic events just north of the first epicentral area. Accordingly, we planned a local geodetic
24 network consisting of five new GNSS (Global Navigation Satellite System) stations located at few km on
25 both sides of the MVFS. This was devoted to picture out, at least partially but in some detail, the possible
26 northward propagation of the crustal ruptures. The building of the stations and a first set of measurements
27 were carried out during a first campaign (September 30th-October 2nd, 2016). On October 26th 2016,
28 immediately north of the epicentral area of the August 24th event, a moderate earthquake ($M_w = 5.9$)
29 indeed occurred, followed four days later (October 30th) by the mainshock ($M_w = 6.5$) of the whole 2016
30 Summer-Autumn seismic sequence. Our local geodetic network was fully affected by the new events and
31 therefore we performed a second campaign soon after (November 11th-13th, 2016). In this brief note, we
32 provide the results of our geodetic measurements that registered the co-seismic and immediately post-
33 seismic deformation of the two major October shocks documenting in some detail the surface deformation
34 close to the fault trace. We also compare our results with the available surface deformation field of the
35 broader area obtained on the basis of the DInSAR technique showing an overall good fit.

37 **2 - Geological framework**

38 The central Apennines are characterized by northeast-verging thrust-propagation folds, involving Mesozoic-
39 Tertiary sedimentary successions. During the 2016 sequence, coseismic deformation was recorded at the
40 rear of the Sibillini Thrust that separates the omonymous mountain chain from the Marche-Abruzzi foothills
41 (Fig. 1). According to many studies in the area affected by the recent earthquakes, the main thrust-related
42 anticlines and associated reverse faults have been dissected and/or inverted by NNW-SSE trending

43 Quaternary normal and oblique-slip faults (Figs. 1 and 2), in particular by the Norcia Fault System (NFS)
44 (Calamita and Pizzi, 1992; Calamita et al., 1982; 1995; 1999; 2000; Blumetti et al., 1990; Blumetti, 1995;
45 Brozzetti and Lavecchia, 1994; Cello et al., 1998; Galadini and Galli, 2000; Pizzi and Scisciani, 2000; Pizzi et
46 al., 2002; **Boncio et al., 2004** Galadini, 2006; Gori et al., 2007) and the Mt. Vettore Fault System (MVFS)
47 (Calamita and Pizzi, 1991; Coltorti and Farabollini, 1995; Cello et al., 1997; Pizzi et al., 2002; Galadini and
48 Galli, 2003; Pizzi and Galadini, 2009) (Figs. 1 and 2). Conversely, Pierantoni et al. (2013) suggest that the
49 major Mt. Sibillini Thrust has been not yet dissected by Quaternary normal faulting though some fresh
50 morphological scarps with free faces in the carbonate bedrock and/or affecting recent slope deposits have
51 been observed and attributed to the local seismic activity.

52 **Within a distance of few tens of kilometers, large evidence of this Quaternary seismotectonic behaviour has**
53 **been provided by several recent earthquakes, like the 1979 Norcia event (M_w 5.9, reactivating the Norcia**
54 **Fault; e.g. Deschamps et al., 2000), the 1984 Gubbio (M_w 5.6, Gubbio Fault; e.g. Boncio et al., 2004), the**
55 **1997 Colfiorito ones (M_w 5.7, 6.0 and 5.6, Calfiorito-Cesi-Costa fault system; e.g. Cello et al., 1997), the**
56 **2009 L'Aquila mainshock and the Campotosto aftershock (M_w 6.3 and 5.4, Upper Aterno Valley-Paganica**
57 **fault system and Gorzano Fault; Blumetti et al. 2013) and basically the same occurred with the 2016**
58 **seismic sequence.**

59 **Surface evidence of the August 24th (e.g., EMERGEO WG, 2016; Livio et al., 2016; Aringoli et al., 2016)**
60 **mainly occurred in the area of the Laga basin (Gorzano Fault), which corresponds to the footwall block of**
61 **Sibillini Thrust, while debated ground ruptures (e.g. Valensise et al., 2016) also occurred in the southern**
62 **sector of the MVFS, which belongs to the hanging-wall block of the orogenic structure. In contrast, as a**
63 **consequence of the mainshock of October 30th, the entire western flank of the Monte Vettore was affected**
64 **by impressive geological effects and clear coseismic ruptures** mapped for a minimum length of 15 km,
65 between the Castelluccio di Norcia and Ussita (EMERGEO WG, 2016) (Fig. 2). The surface ruptures occurred
66 along distinct fault splays of the fracture system. For example, along the western slope of Monte Vettore
67 three main west dipping splays were activated together with two antithetic branches (Figs. 1 and 2). The
68 observed vertical offset reached 2 m along the main west dipping fault segment, where the slickensides
69 show a prevalent dip-slip component of motion. Vertical displacements of a few centimetres were also
70 recorded along an antithetic surface rupture bordering to the west the Castelluccio plain, about 6-7 km far
71 from the main ground rupture possibly connected to a secondary fault (Figs. 1B and 2).

72 **It is worth to note that August-October earthquakes occurred in a sector of the Central Apennines**
73 **characterized by high geodetic strain-rates (e.g., Devoti et al., 2011; D'Agostino 2014), where several**
74 **continuous GNSS stations are operating.**

75

76 **Implementation and Analysis of UNICT discrete GNSS stations**

77 Following the August, 24th, M_w 6.0 earthquake, the GEOMATIC Working Group of the Catania University
78 (UNICT) in collaboration with the SpinOff EcoStat s.r.l. and researches of the Ferrara University, started a
79 detailed monitoring of ground deformation in the epicentral area using the Global Navigation Satellite
80 System (GNSS) technique. **The GNSS measurement has been made in static mode, setting the time at 6**
81 **hours and post-processing position, in order to reduce tropospheric error and using IGS precise products**
82 **for orbits. The IGS station coordinates were kept fixed in order to align the final velocity field with the**
83 **WGS84 reference frame. The measurement mode, adopted for receiver-satellite range determination, is**
84 **performed with a double frequency receiver, allowing phase and code measurements on the signal carrier**
85 **(L1, L2, C1, P1, P2, S1, S2). The coordinates estimation is based on the principle of minimum squares.**

86 For this aim, five GNSS stations have been installed on **new benchmarks purposely** built by the working
87 group and here referred to as UNICT network (Fig. 3). These new stations have been realized taking into
88 account the following criteria:

- 89 I. the distribution of the existing permanent and discrete measurement benchmarks belonging to
90 different networks that were active before the event of 24 August (IGM; RING; CAGEONET; DPC;
91 ISPRA) (Fig. 2B).
- 92 II. the seismotectonic setting of the area in relation to the macroseismic data and to the reactivated
93 structures (Figs. 1 and 2);
- 94 III. surface and deep geometry of the major faults related to tectonic setting (Fig. 1B).
- 95 IV. the **lack of possible gravitational** instabilities in both static and dynamic conditions in sites where
96 the new benchmarks are built.

97 Based on the above criteria, the working group installed the benchmarks at the bottom of both western
98 and eastern slopes of Mt. Vettore, within an area about 8 km-long and 5 km-wide in the N-S and E-W
99 directions, respectively. The distribution of the benchmarks was planned for depicting the principal
100 deformation zone developed as a consequence of the August 24th, event (Fig 2 and 3) and particularly with
101 points:

- 102 I. much closer to the epicentral area than the already existing ones belonging to other networks
103 (Fig. 2B);
- 104 II. characterized by equivalent distances from the reactivated Mt. Vettore Fault segments (Fig. 2);
- 105 III. within a distance of 30 km from the closest permanent network points that have been not affected
106 by deformation, therefore allowing a rigorous elaboration during the post processing phases (Fig.
107 3).

108 The realization of GNSS monument on the UNICT benchmarks consists of the following steps:

- 109 I. selection of a suitable point, corresponding to a massive rocky outcrop or a man-made monument
110 with foundation; these sites must be also free of structures or other natural elements in the
111 surroundings that may constitute a perturbation during recording;
- 112 II. testing of GNSS signal reception by short-term exams, and control of parameters set by the quality
113 check carried out by software TEQC ([http://www.unavco.org/software/data-
114 processing/teqc/teqc.html](http://www.unavco.org/software/data-processing/teqc/teqc.html));
- 115 III. implementation of the hole for housing the bushing and check of its verticality; the hole has a
116 diameter of 35 mm and a depth of 100 mm, it is realized through small-sized battery-powered
117 equipment (Makita DHR243 hammer drill) (Fig. 3);
- 118 IV. fixing and anchoring of the knurled steel bushing (length 67 mm and diameter 20 mm), with bi-
119 component resins or quick-setting cements (Fig. 3);
- 120 V. following the cementation to the artefact or to rocky outcrop, a male-male threaded bar can be
121 screwed in until end of stroke; the height could be variable and this fact will be considered in the
122 data processing. We have used a threaded bar 670 mm-high. (Fig. 3).

123 The GNSS monument is thus completed with a GNSS receiver TOPCON, mounting a HiPer V antenna,
124 characterized by 226 channels and position accuracy with band L1+L2 in Static mode of 3 mm + 0.1 ppm
125 (horizontal) and 3.5 mm + 0.4 ppm (vertical). All registrations last six hours in static mode.

126 Following the August 24th event, at the end of September 2016 the working group have started the first
127 survey campaign with the installation of five UNICT benchmarks: two stations **were** located east of the Mt.

128 Vettore fault (VTE1,VTE2), the other three (VTW3,VTW4, VTW5) west of the fault (Figs. 4 and 5). During
 129 November 2016 (*i.e.* after the October 30th event), a second field campaign was carried out following the
 130 same procedure and using the same instrumentation. The second set of measurements allowed recording
 131 the co-seismic displacement caused by both the M_w 5.9 and M_w 6.5 events of October 26th and 30th,
 132 respectively (doy (day of year) 2016/274 and doy 2016/318).

133 The data from survey-mode GNSS stations have been downloaded and processed using TOPCON Magnet
 134 analysis software evaluating co-seismic solution and comparing with AUSPOS web-based online services for
 135 GPS data processing (Ocalan et al., 2013), whose engine is based on Bernese 5.2 software. In the software
 136 TOPCON, the baseline is automatically created for any pair of static occupations, where we set up six hours
 137 for Minimum Duration and the baselines max length of 50 km, cut-off angle of 15°, troposphere model
 138 Goad-Goodman and, finally, meteo model NRLMSISE (neutral temperature and densities in Earth's
 139 atmosphere).

140 For the analyses we referred to the measurement of a stable reference frame of five GNSS stations
 141 belonging to the RING (Rete Integrata Nazionale GPS) network, with a maximum baseline length of 50 km
 142 using stations CESI, GNAL, GUMA, MTER and MTTO (Figs. 4 and 5). Data processing has been carried out
 143 with adjustment by Least Squares and a TAU Criterion.
 144

ID	Station	Longitudine	Latitudine	disp _{N-S}	disp _{E-W}	disp _{UP}	unc _{N-S}	unc _{E-W}	unc _{UP}
VTE1	FOCE_SENTIERO	13° 15' 57,45166"	42° 51' 57,04340"	141	312	29	15.5	16.5	44.0
VTE2	PRETARE	13° 16' 33,20959"	42° 47' 56,56780"	60	282	67	19.0	16.5	46.0
VTW3	QUARTUCCIOLO	13° 14' 46,41153"	42° 47' 56,57032"	198	26	-349	15.5	14.5	36.0
VTW4	COLLE_CURINA	13° 13' 55,01245"	42° 48' 59,62491"	102	288	-769	15.5	15.0	36.0
VTW5	CASTELLUCCIO_VALLE	13° 12' 56,20423"	42° 49' 54,89014"	353	418	-707	15.0	13.5	37.5

145
 146 *Tab 1 - Three components co-seismic displacements and relative uncertainties estimated for the GNSS stations of the*
 147 *UNICT network. Coordinates are WGS84 east and north, respectively. All displacement and uncertainty values are in*
 148 *millimeters. For all stations, the cut-off angle is 15°, the troposphere model is the Goad-Goodmar and the meteo model*
 149 *used is NRLMSISE. The table can be download as ASCII file on the INGVRING web page (<http://ring.gm.ingv.it>).*

150
 151 **Concluding remarks**

152 Using the GNSS technique we investigated the ground deformation that occurred in the surroundings of the
 153 Mt. Vettore Fault System. This foresight action allowed us to record the co-seismic and part of the post-
 154 seismic deformation of the second (strongest) events (M_w 5.9 and M_w 6.5) on October 26th and October
 155 30th, 2016 respectively. Taking into account the geometry of the fault system in the broader epicentral area
 156 and following the stress-triggering concept (Stein et al., 1999; Steacy et al., 2005), we have identified a
 157 potential fault zone most vulnerable to future seismic events just north of the fault segment reactivated
 158 during the August 24th earthquake (Figs. 2B and 5). With this in mind, in order to measure the post seismic
 159 deformation and to possibly record the potential migration of the co-seismic process, we selected some
 160 sites and built five new GNSS benchmarks, distributed east and west of the northern-central segment of the
 161 Mt. Vettore Fault System. For site selection we also considered the presence and distribution of other
 162 benchmarks located before the second seismic event by other research groups (IGM; RING; CAGEONET;
 163 DPC; ISPRA). The epicentral location of the October events eventually confirmed our guess and we then
 164 performed soon after a second campaign of measurements for quantifying the relative motion of the
 165 stations.

166 The measured deformation (with 95% confidence errors) is characterised by both horizontal and vertical
 167 movements. In particular, the east benchmark VTE1 documents 312 mm of eastward horizontal

168 displacement and 29 mm of upward motion, while the VTE2 282 mm of eastward horizontal displacement
169 and 67 mm of upward component of motion. On the contrary, all three western benchmarks recorded
170 westward horizontal displacements (419, 288 and 26 mm) and subsidence (707, 288 and 769 mm) for
171 stations VTW5, VTW4 and VTW3, respectively. In conclusion, we documented ca. 730 mm of ENE-WSW
172 lengthening on a distance of 7 km in correspondence of the northern sector of the Mt. Vettore Fault
173 Segment, while the off-fault vertical displacement between footwall and hanging-wall blocks was 736 mm.
174 We also compared our results with the displacement distribution obtained by other research group with
175 DInSAR techniques, recorded between October 26th 2016 (pre-event images) and November 1st 2016
176 (post-event images), and other GNSS stations, active before the second seismic event. In Fig. 5 we may
177 observe the overall consistency of the different approaches and datasets.

178
179

180 **Acknowledgments** This paper was carried out with the financial support of the University of Catania (FIR
181 2014 Project Code 2C7D79, Scientific Supervisor: G. De Guidi) and University Spin Off of Catania EcoStat
182 s.r.l.

183
184

185 **References**

- 186 Anzidei M., Baldi P. and Serpelloni E. (2008). The coseismic ground deformations of the 1997 Umbria-
187 Marche earthquakes: A lesson for the development of new GPS networks, *Ann. Geophys.*, 51(2–3), 27–
188 43.
- 189 Anzidei M. and Pondrelli S. (Eds) (2016). The Amatrice seismic sequence: preliminary data and results,
190 *Annals of Geophysics*, 59, Fast Track 5, 2016
- 191 Aringoli D., Farabollini P., Giacompetti M., Materazzi M., Paggi S., Pambianchi G., Pierantoni P.P., Pistolesi E.,
192 Pitts A. and Tondi E. (2016). The August 24th 2016 Accumoli earthquake: surface faulting and Deep-
193 Seated Gravitational Slope Deformation (DSGSD) in the Monte Vettore area. *Ann. Geophysics*, 59, fast
194 track 5, 2016; doi: 10.4401/ag-7199.
- 195 Blumetti A.M. (1995). Neotectonic investigations and evidence of paleoseismicity in the epicentral area of
196 the January-February 1703, Central Italy, earthquakes. In: Serva, L. & Slemmons, D. B., (eds.):
197 Perspectives in paleoseismology. Association of Engineering Geologists, spec. publ. 6, 83-100.
- 198 Blumetti A.M., Dramis F., Gentili B. and Pambianchi G. (1990). La struttura di M. Alvagnano-Castel Santa
199 Maria nell'area nursina: aspetti geomorfologici e sismicità storica. *Rend. Soc. Geol. It.*, 13, 71-76.
- 200 Blumetti A.M., Guerrieri L. and Vittori E. (2013). The primary role of the Paganica-San Demetrio fault system
201 in the seismic landscape of the Middle Aterno Valley basin (Central Apennines). *Quaternary*
202 *International*, 288, 183-194, doi: 10.1016/j.quaint.2012.04.040.
- 203 Boncio P., Lavecchia G., and Pace B (2004). Defining a model of 3D seismogenic sources for Seismic Hazard
204 Assessment applications: The case of central Apennines (Italy). *Journal of Seismology* 8: 407–425.
- 205 Brozzetti F. and Lavecchia G. (1994). Seismicity and related extensional stress field; the case of the Norcia
206 seismic zone (central Italy). *Annales Tectonicae* 8, 36–57
- 207 Calamita F. and Pizzi A., 1992. Tettonica quaternaria nella dorsale appenninica umbro-marchigiana e bacini
208 intrappenninici associati. *Studi Geologici Camerti*, spec. vol. 1992/1, 17-25.
- 209 Calamita F., Coltorti M., Deiana G., Dramis F. and Pambianchi G. (1982). Neotectonic evolution and
210 geomorphology of the Cascia and Norcia depression (Umbria-Marche Apennine). *Geografia Fisica e*
211 *Dinamica Quaternaria*, 5, 263-276.

212 Calamita F., Pizzi A., Romano A., Roscioni M., Scisciani V. and Vecchioni G. (1995). La tettonica quaternaria
213 nella dorsale appenninica umbro-marchigiana: una deformazione progressiva non coassiale. Studi
214 Geol. Camerti, vol. spec.1995/1, 203-223.

215 Calamita F., Coltorti M., Pieruccini P. and Pizzi A. (1999). Evoluzione strutturale e morfogenesi plio-
216 quaternaria dell'appennino umbro-marchigiano tra il preappennino umbro e la costa adriatica.
217 Bollettino della Società Geologica Italiana, 118, 125-139.

218 Calamita F., Coltorti M., Piccinini D., Pierantoni P.P., Pizzi A., Ripepe M., Scisciani V. and Turco E. (2000).
219 Quaternary faults and seismicity in the Umbro-Marchean Apennines (central Italy). Journal of
220 Geodynamics 29, 245–264.

221 Cello G., Mazzoli S., Tondi E. and Turco E. (1997). Active tectonics in the Central Apennines and possible
222 implications for seismic hazard analysis in peninsular Italy. Tectonophysics, 272, 43-68.

223 Cello G., Deiana G., Mangano P., Mazzoli S., Tondi E., Ferrelli L., Maschio L., Michetti A.M., Serva L. and
224 Vittori E. (1998). Evidence for surface faulting during the September 26, 1997, Colfiorito (Central Italy)
225 earthquakes. Journal of Earthquake Engineering, 2, 1-22.

226 Coltorti M. and Farabollini P. (1995). Quaternary evolution of the Castelluccio di Norcia Basin. Il
227 Quaternario, 8, 149-166.

228 Deschamps A., Courboulex F., Gaffet S., Lomax A., Virieux J., Amato A., Azzara A., Castello B., Chiarabba C.,
229 Cimini G.B., Cocco M., Di Bona M., Margheriti L., Mele F., Selvaggi G., Chiaraluce L., Piccinini D. and
230 Ripepe M. (2000). Spatio-temporal distribution of seismic activity during the Umbria-Marche crisis,
231 1997. Journal of Seismology 4: 377–386.

232 Devoti R., Esposito A., Pietrantonio G., Pisani A.R. and Riguzzi F. (2011). Evidence of large scale deformation
233 patterns from GPS data in the Italian subduction boundary. Earth and Planetary Science Letters, 311,
234 230–241, doi:10.1016/j.epsl.2011.09.034.

235 EMERGEO W.G. (2016). Coseismic effects of the 2016 Amatrice seismic sequence: first geological results.
236 Ann. Geophysics, 59, fast track 5, 2016; doi: 10.4401/ag-7195

237 Galadini F. and Galli P. (2000). Active tectonics in the Central Apennines (Italy) - Input data for seismic
238 hazard Assessment. Natural Hazards, 22, 225-270.

239 Galadini F. and Galli P. (2003). Paleoseismology of silent faults in the central Apennines (Italy): the Mt.
240 Vettore and Laga Mts. faults. Annali di Geofisica, 46, 815-836.

241 Galvani A., Anzidei M., Devoti R., Esposito A., Pietrantonio G., Pisani A., Riguzzi F. and Serpelloni E. (2012).
242 The interseismic velocity field of the central Apennines from a dense GPS network. Ann. Geophys. 55,
243 5, 2012; doi: 10.4401/ag-5634.

244 Gori S., Dramis F., Galadini F. and Messina P. (2007). The use of geomorphological markers in the footwall
245 of active faults for kinematic evaluations: examples from the central Apennines. Bollettino della
246 Società Geologica Italiana, 126, 365-374.

247 GdL-INGV (Gruppo di Lavoro INGV sul terremoto in centro Italia) (2016). Summary report on the October
248 30, 2016 earthquake in central Italy Mw 6.5, doi: 10.5281/zenodo.166238

249 Harris R.A. (1998). Introduction to special section: Stress triggers, stress shadows, and implications for
250 seismic hazard. J. Geophys. Res. 103, 347–358.

251 Kilb D., Gomberg J. and Bodin P. (2000). Triggering of earthquake aftershocks by dynamic stresses. Nature
252 408, 570–574.

253 Livio F., Michetti A.M., Vittori E., Gregory L., Wedmore L., Piccardi L., Tondi E., Roberts G. and Central Italy
254 Earthquake Working Group (2016): Surface faulting during the August 24, 2016, Central Italy
255 earthquake (Mw 6.0): preliminary results. Ann. Geophysics, 59, fast track 5, 2016; doi: 10.4401/ag-
256 7197

- 257 Ocalan T., Erdogan B., Tunalioglu N. (2013). Analysis of web-based online services for GPS relative and
 258 precise point positioning techniques. *Bol. Ciênc. Geod., sec. Artigos, Curitiba, v. 19, no 2, p.191-207,*
 259 *abr-jun, 2013*
- 260 Mantovani E., Viti M., Babbucci D., Cenni N., Tamburelli C., Vannucchi A., Falciani F., Fianchisti G., Baglione
 261 M., D'Intinosante V. and Fabbroni P. (2011). Sismotettonica dell'Appennino Settentrionale. Implicazioni
 262 per la pericolosità sismica della Toscana. Regione Toscana, Centro stampa Giunta Regione Toscana,
 263 Firenze, pagg. 88 (<http://www.rete.toscana.it/sett/pta/sismica/index.shtml>).
- 264 Pierantoni P., Deiana G. and Galdenzi S. (2013). Stratigraphic and structural features of the Sibillini
 265 mountain (Umbria-Marche- Appennines, Italy). *Ital. J. Geosci. (Boll. Soc. Geol. It.) Vol.132 No.3, pp.*
 266 *497-520.*
- 267 Pizzi A. and Galadini F. (2009). Pre-existing cross-structures and active fault segmentation in the northern-
 268 central Apennines (Italy), *Tectonophysics, 476(1-2), 304–319, doi:10.1016/j.tecto.2009.03.018.*
- 269 Pizzi A. and Scisciani V. (2000). Methods for determining the Pleistocene–Holocene component of
 270 displacement on active faults reactivating pre-Quaternary structures: examples from the central
 271 Apennines (Italy). *Journal of Geodynamics 29, 445–457.*
- 272 Pizzi A., Calamita F., Coltorti M. and Pieruccini P. (2002). Quaternary normal faults, intramontane basins
 273 and seismicity in the Umbria-Marche- Abruzzi Apennine ridge (Italy): contribution of neotectonic
 274 analysis to seismic hazard assessment. *Boll. Soc. Geol. It., Spec. Publ., 1, 923–929.*
- 275 Pizzi A., Calamita F., Coltorti M. and Pieruccini P. (2002). Quaternary normal faults, intramontane basins
 276 and seismicity in the Umbria-Marche- Abruzzi Apennine ridge (Italy): contribution of neotectonic
 277 analysis to seismic hazard assessment. *Boll. Soc. Geol. It., Spec. Publ., 1, 923–929.*
- 278 Pizzi A. and Galadini F. (2009) Pre-existing cross-structures and active fault segmentation in the northern-
 279 central Apennines (Italy). *Tectonophysics. 476, 304-319.*
- 280 Steacy S., Gombert J. and Cocco M. (2005). Introduction to special section: Stress transfer, earthquake
 281 triggering, and time-dependent seismic hazard. *J. Geophys. Res. 110, B05S01.*
- 282 Stein R.S. (1999). The role of stress transfer in earthquake occurrence. *Nature 402, 605–609.*
- 283 Valensise G., Vannoli P., Basili R., Bonini L., Burrato P., Carafa M.C., Fracassi U., Kastelic V., Maesano F.E.,
 284 Tiberti M. and Tarabusi G. (2016). Fossil landscapes and youthful seismogenic sources in the central
 285 Apennines: excerpts from the 24 August 2016, Amatrice earthquake and seismic hazard implications.
 286 *Ann. Geophysics, 59, fast track 5, 2016; doi: 10.4401/ag-7215.*

287

288 Website links

289 <http://iside.rm.ingv.it>

290 <http://ring.gm.ingv.it>

291 <http://www.igmi.org/geodetica/>

292 [http://www.irea.cnr.it/index.php?option=com_k2&view=item&id=761:nuovi-risultati-sul-terremoto-del-](http://www.irea.cnr.it/index.php?option=com_k2&view=item&id=761:nuovi-risultati-sul-terremoto-del-30-ottobre-2016-ottenuti-dai-radar-dei-satelliti-sentinel-1)
 293 [30-ottobre-2016-ottenuti-dai-radar-dei-satelliti-sentinel-1](http://www.irea.cnr.it/index.php?option=com_k2&view=item&id=761:nuovi-risultati-sul-terremoto-del-30-ottobre-2016-ottenuti-dai-radar-dei-satelliti-sentinel-1)

294 [http://www.irea.cnr.it/index.php?option=com_k2&view=item&id=761:nuovi-risultati-sul-terremoto-del-](http://www.irea.cnr.it/index.php?option=com_k2&view=item&id=761:nuovi-risultati-sul-terremoto-del-30-ottobre-2016-ottenuti-dai-radar-dei-satelliti-sentinel-1)
 295 [30-ottobre-2016-ottenuti-dai-radar-dei-satelliti-sentinel-1](http://www.irea.cnr.it/index.php?option=com_k2&view=item&id=761:nuovi-risultati-sul-terremoto-del-30-ottobre-2016-ottenuti-dai-radar-dei-satelliti-sentinel-1)

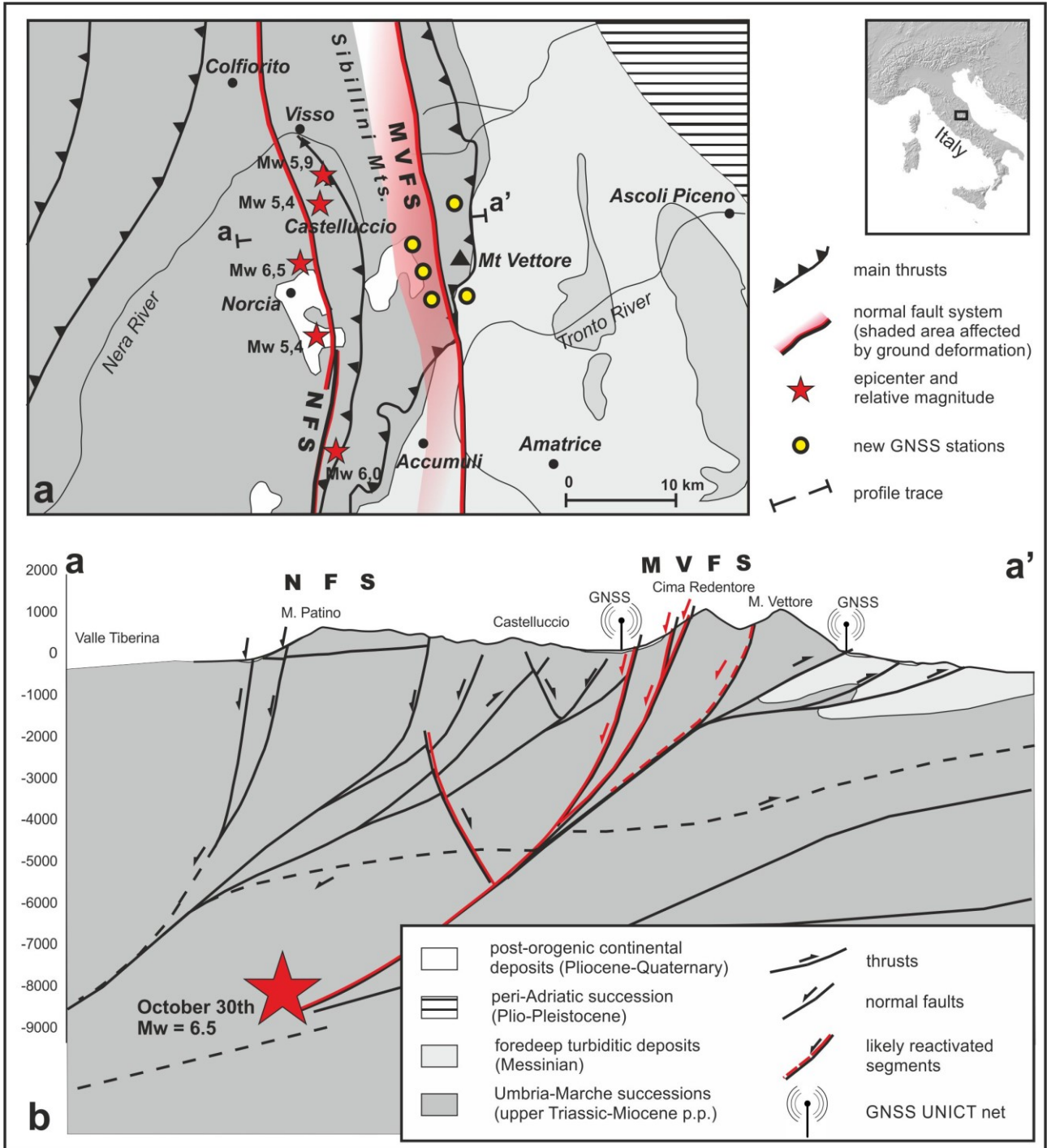
296 <http://www.isprambiente.gov.it>

297 <http://www.unavco.org/software/data-processing/teqc/teqc.html>

298 Rete Integrata Nazionale GPS - <http://ring.gm.ingv.it/>

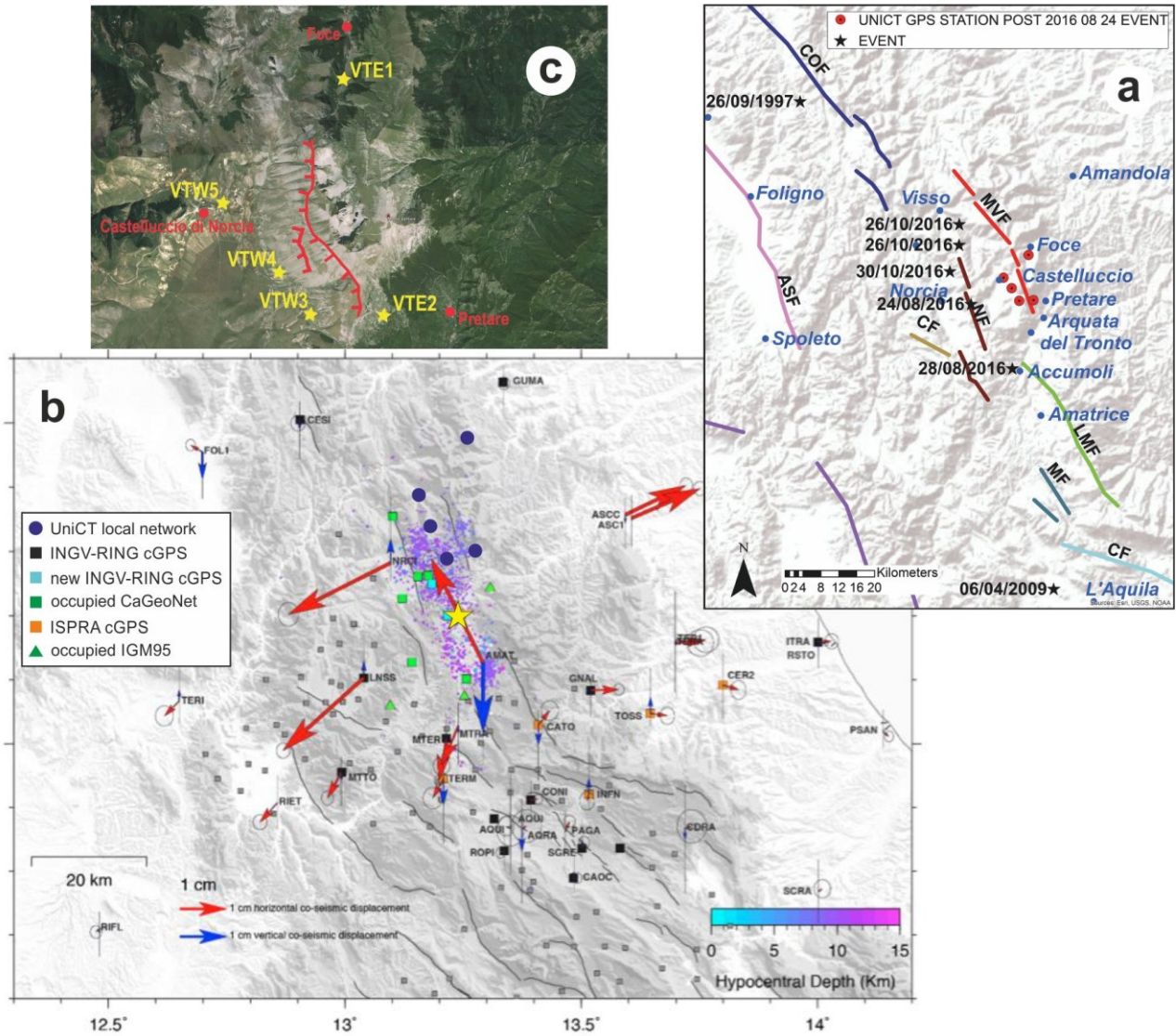
299 [http://terremoti.ingv.it/it/ultimi-eventi/1001-evento-sismico-tra-le-province-di-rieti-e-ascoli-p-m-6-0-24-](http://terremoti.ingv.it/it/ultimi-eventi/1001-evento-sismico-tra-le-province-di-rieti-e-ascoli-p-m-6-0-24-agosto.html)
 300 [agosto.html](http://terremoti.ingv.it/it/ultimi-eventi/1001-evento-sismico-tra-le-province-di-rieti-e-ascoli-p-m-6-0-24-agosto.html); Sequenza sismica di Amatrice, Norcia, Visso: approfondimenti e report scientifici

301



303
304
305
306
307
308

Fig. 1 Simplified seismotectonic map of central Apennines (a) and geological profile across the epicentral area (b). The location of the major event (October 30th) is from GdL INGV (2016), while the main geostructural features from Pierantoni et al., (2013) and Mantovani et al., (2011) modified).



310
 311 *Fig. 2 – a) Digital Elevation Model with shaded relief of central Apennines showing the active fault system and the*
 312 *major events since 1997 (ASF: Assisi Fault; COF: Colfiorito Fault; CF: Cascia Fault; MVF: Mt. Vettore Fault; NF: Norcia*
 313 *Fault; LMF: Laga Mts. Fault; MF: faults of the Montereale basin). b) Horizontal (red arrows) and vertical (blue arrows)*
 314 *consensus co-seismic displacements (with 68% confidence errors), and the local UniCT GNSS network. The aftershocks*
 315 *of the August 24th, Mw 6.0 main event (yellow star) are colored as a function of depth (from <http://iside.rm.ingv.it>); c).*
 316 *GoogleEarth map showing the new five GNSS stations (yellow stars) located in the near field of, and surrounding, the*
 317 *October 30th coseismic ground ruptures (red lines).*
 318

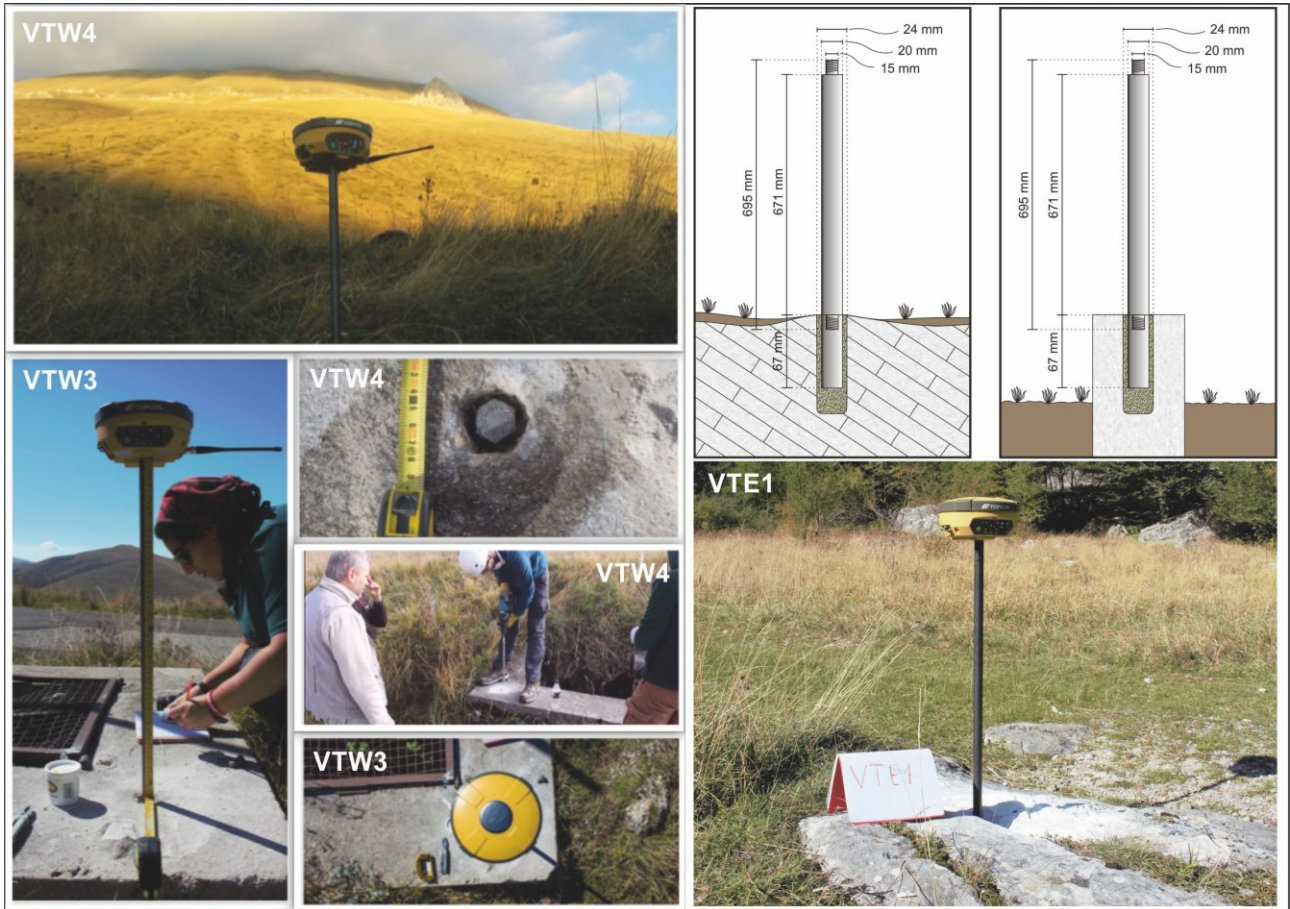
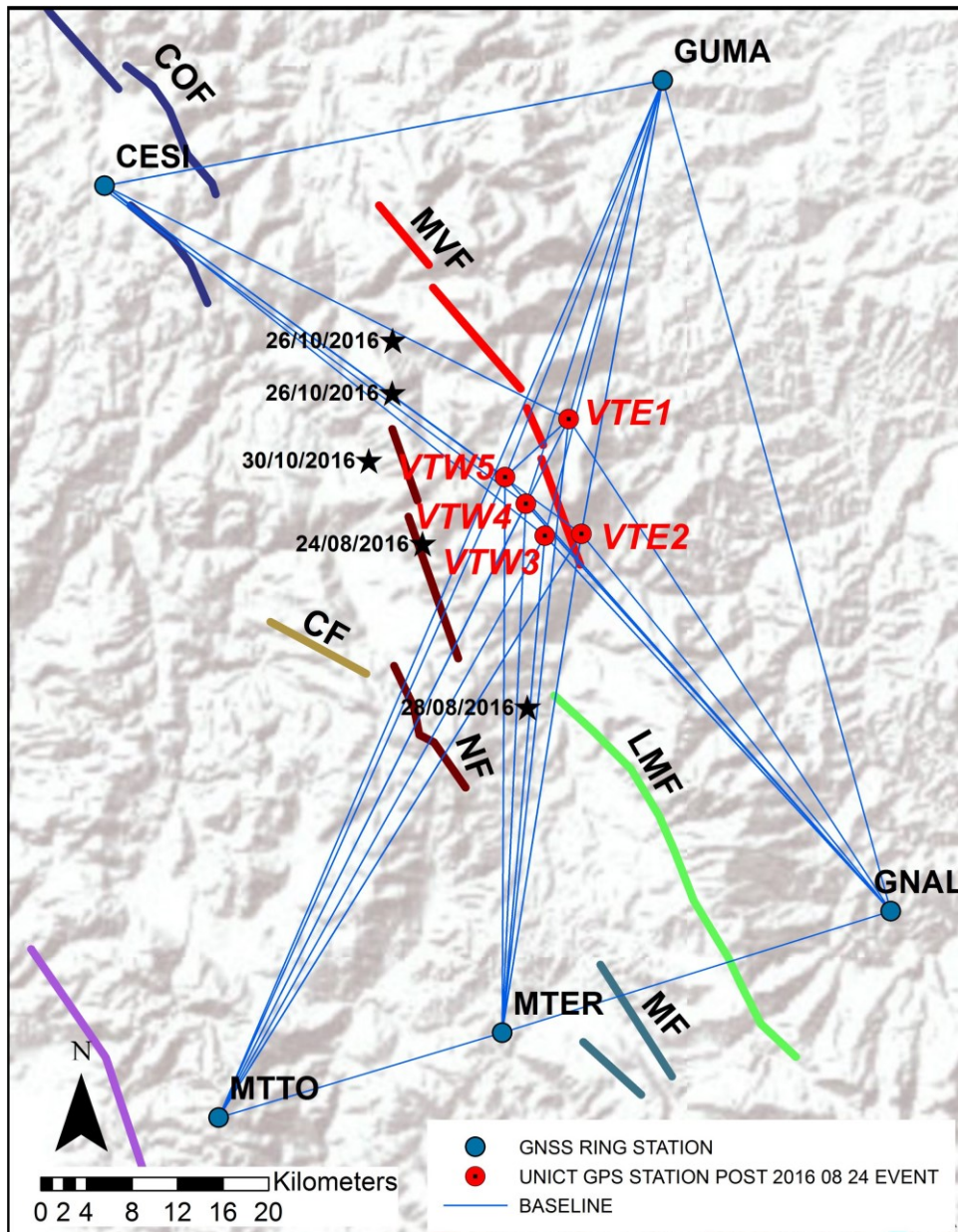


Fig. 3 Synoptic picture showing installation of the new GNSS stations, measurement and processing phases.



324

325 **Fig. 4** Baselines obtained by combining the new GNSS UNICT stations with selected GNSS ones from the RING Network.

326

327

328

329

330

331 **Fig. 5** Color-coded maps showing the E-W (a) and vertical (b) displacement distribution obtained by the DInSAR
 332 technique (http://www.irea.cnr.it/index.php?option=com_k2&view=item&id=761:nuovi-risultati-sul-terremoto-del-30-ottobre-2016-ottenuti-dai-radar-dei-satelliti-sentinel-1) recorded On October 26th 2016 (pre-event images) and on
 333 November 1st 2016 (post-event images). The red and blu arrows represent the consensus pre-, co-, and post-seismic
 334 displacements (with 95% confidence errors) on the basis of the GNSS UNICT network. Epicenters of major shocks are
 335 from <http://ring.gm.ingv.it>.

337

